



Dyke-impounded fresh groundwater resources in coastal and island volcanic aquifers: Learning from the Canary Islands (Spain)

Miguel Ángel Marazuela^{a,*}, Carlos Baquedano^a, Noelia Cruz-Pérez^b, Jorge Martínez-León^a, Chrysi Laspidou^c, Juan Carlos Santamarta^b, Alejandro García-Gil^{a,*}

^a Geological Survey of Spain (IGME), Spanish National Research Council (CSIC), Ríos Rosas 23, 28003 Madrid, Spain

^b Department of Agricultural and Environmental Engineering, University of La Laguna (ULL), Ctra. Geneto 2, 38200 La Laguna, Spain

^c Department of Civil Engineering, University of Thessaly, 38334 Volos, Greece

ARTICLE INFO

Editor: Damia Barcelo

Keywords:

Volcanic dyke
Island aquifer
Seawater intrusion
Freshwater lens
Drinking water
Numerical modeling

ABSTRACT

Freshwater in coastal and island aquifers is a valuable resource whose availability is strongly conditioned by heterogeneity. More than 80 % of the Earth's surface is of volcanic origin, but the effect of volcanic dykes on the geometry of the saline interface that separates freshwater from seawater is still underexplored. This paper analyzes the impact of volcanic dykes on the depth of the saline interface in coastal and island aquifers and, subsequently, on the availability of fresh groundwater. Hydrogeological and hydrochemical data from a gallery, perpendicularly crossing several tens of dykes, were integrated with numerical modeling on the volcanic island of *El Hierro* (Canary Islands, Spain). Measured hydraulic heads demonstrated that the presence of dykes increased the hydraulic gradient by more than an order of magnitude, with respect to an adjacent area not affected by dykes. Numerical assessment confirmed that the lower the hydraulic conductivity of the dykes, the greater the depth of the saline interface inland. This impact led to fresh groundwater reserves increasing inland, relative to a hypothetical case without dykes. Numerical simulations also demonstrated that dykes can prevent salinization of production wells in coastal and island aquifers, if they are correctly located. Locating production wells far enough inland in an area affected by dykes allowed a higher freshwater extraction rate than if dykes did not exist; near the coastline, the effect tended to be the opposite. These results will be key to improving the management of fresh groundwater resources in coastal volcanic aquifers, and especially on volcanic islands such as the Hawaiian Islands or the Macaronesian archipelagos.

1. Introduction

Freshwater in coastal areas, and especially on islands, is a scarce and highly valuable resource whose abundance and quality are strongly influenced by geological heterogeneity (Bear et al., 1999; Cao et al., 2021; Folch et al., 2020; García-Gil et al., 2022; Hernández Ríos et al., 2023; Leoni et al., 2021; Lopes et al., 2022; Marazuela et al., 2022; Martínez-Pérez et al., 2022; Parizi et al., 2019; Weymer et al., 2022). Most of the islands have a limited amount of surface storage potential to capture freshwater (streams and lakes are scarce or non-existent), and freshwater lenses from aquifers are key to guaranteeing the supply of drinking, industrial and agricultural water (Bedekar et al., 2019; Stoeckl and Houben, 2012; Werner et al., 2017).

The depth of the saltwater that naturally underlies freshwater resources in coastal and island aquifers is critical to estimating well yield

and avoiding well salinization due to seawater intrusion (Geng and Michael, 2020; Izuka and Gingerich, 1998; Post et al., 2019, 2018a; Schmork and Mercado, 1969; Werner et al., 2013; Yu and Michael, 2019). Intensive pumping can cause the freshwater-seawater saline interface to rise into the pumped well, resulting in increased sodium and chloride concentrations (Houben and Post, 2017). Although pioneering studies on coastal aquifers assumed homogeneous aquifers (Fetter Jr., 1972; Glover, 1959), the impact of heterogeneity on the depth and geometry of the saline interface has been widely demonstrated since then (Abarca et al., 2007; Etsias et al., 2021; Houben et al., 2018; Kreyns et al., 2020; Mahmoodzadeh and Karamouz, 2019; Marazuela et al., 2020, 2018; Muallem and Bear, 1974; Sebben et al., 2015; Simmons et al., 2001; Stoeckl et al., 2015; Younes and Fahs, 2015). This has even led to the investigation of preventive and corrective measures for seawater intrusion based on subsurface dams or artificial modifications

* Corresponding authors.

E-mail addresses: ma.marazuela@igme.es (M.Á. Marazuela), a.garcia@igme.es (A. García-Gil).

<https://doi.org/10.1016/j.scitotenv.2023.165638>

Received 26 May 2023; Received in revised form 26 June 2023; Accepted 16 July 2023

Available online 18 July 2023

0048-9697/© 2023 The Authors. Published by Elsevier B.V. This is an open access article under the CC BY license (<http://creativecommons.org/licenses/by/4.0/>).

of hydraulic conductivity (Chang et al., 2020; Santamarta and Hernández-Sánchez, 2007; Strack et al., 2016). However, most research published to date on seawater intrusion in highly heterogeneous aquifers has focused on anisotropic/layered sedimentary systems, fractured systems and karstic systems (e.g., Giese and Barthel, 2021; Simmons et al., 2001); volcanic dykes are still underexplored.

More than 80 % of the Earth's surface - above and below sea level - is of volcanic origin, which makes volcanic dykes a very frequent structure in coastal aquifers (Comte et al., 2017; Vázquez-Suñé et al., 2016) and island aquifers (Becerril et al., 2013; Ecker, 1976; Izuka et al., 2018). Dykes are sub-vertical sheeted intrusions, which generally intrude into extensional faults and fractures during the later stages of the volcanic cycle. Although weathered dykes can act as preferential groundwater flow paths when surrounded by less permeable host rock, most of the time dykes act as flow barriers, leading to compartmentalization and stepwise hydraulic heads (Custodio, 2007; Perrin et al., 2011; Santamarta et al., 2010; Takasaki and Mink, 1985). For example, this barrier effect has been demonstrated to be critical for the construction of underground civil infrastructure in cities (Font-Capó et al., 2012, 2011). Focusing on islands, the Hawaiian Islands and the Macaronesian archipelagos (Canary Islands, Azores, Madeira, Cape Verde) constitute examples of islands where groundwater flow is strongly influenced by the presence of dykes (Ecker, 1976; Fernandes et al., 2020; Izquierdo, 2014; Izuka et al., 2018; Lachassagne et al., 2014; Santamarta, 2017; Scholl et al., 1996). In a study carried out on Tenerife Island (Canary Islands, Spain), Ecker (1976) observed that groundwater compartments that are irregular in volume, shape, and structure develop in areas affected by dykes. Takasaki and Mink (1985) concluded that groundwater levels in the marginal dyke zones of O'ahu (Hawaii) stand hundreds of feet higher than they would without the dykes, thereby increasing the volume of stored fresh groundwater by hundreds of billions of gallons. Using physical experiments and numerical modeling, Houben et al. (2018) confirmed that dykes lead to an impoundment of fresh groundwater and a compartmentalization of the aquifer. In a study carried out on the coast of Belfast (Northern Ireland, United Kingdom), Comte et al. (2017) concluded that freshwater inflows from upland recharge areas concentrate on the land-facing side of the dykes and saltwater penetration is higher on their sea-facing side, similar to what happens with subsurface dams (Chang et al., 2020).

However, to the best of our knowledge, there are no studies that have directly analyzed the impact of dykes on the availability of fresh groundwater in coastal and island aquifers and how they condition the extraction of this resource. This is probably accentuated by the scarcity of structures perpendicularly traversing dyke-impounded fresh groundwater resources along which its impact can be assessed. Understanding how drinking water supply systems can benefit from the effect of dykes to prevent salinization from seawater intrusion and achieve maximum well yield is key to guaranteeing the future of many islands globally, such as the Hawaiian Islands or the Macaronesian archipelagos, which have seen most of their wells abandoned due to low yield or salinization in the last decades (Custodio et al., 2016; Ecker, 1976; Izuka et al., 2018; Santamarta and Rodríguez-Martín, 2020).

This paper analyzes the effect of volcanic dykes on the quantity and quality of freshwater resources in coastal and island aquifers through the first study that integrates in situ hydrogeological and hydrochemical data and numerical modeling. To reach this objective, a synthetic numerical model reproducing the density-driven groundwater flow and salt transport across a vertical profile, perpendicular to the sea and strongly affected by dykes, was built based on the *Los Padrones* well-gallery on the volcanic island of *El Hierro* (Canary Islands, Spain) and compared with in-situ field data. This outstanding hydraulic infrastructure that crosses several tens of dykes along its >1 km length supplies 37 % of the island's water demand, and the hydraulic and hydrochemical data obtained along it allowed analysis of the impact of dykes on fresh groundwater resources. The results of this study will contribute to the management and exploitation of fresh groundwater

resources in coastal aquifers and volcanic islands.

2. Materials and methods

2.1. Study area

The island of *El Hierro* is the youngest (1.12 Ma), smallest (268.71 km²), and southwesternmost of the Canary Islands (Spain), which are located in the Atlantic Ocean, near North Africa (García-Gil et al., 2023; IGME, 1997a, 1997b, 1997c, 1997d; Troll and Carracedo, 2016) (Fig. 1). *El Hierro* is also the least populated island (11,423 inhabitants in 2022) and 60 % of its surface area is protected (UNESCO Biosphere Reserve). The climate of each area of the island is determined by its orography (maximum altitude 1501 m a.s.l. in *Pico de Malpaso*) and the influence of trade winds and ocean currents that humidify what would otherwise be a predominantly sub-desert climate. The average rainfall is 393.7 mm/a, with an average aquifer recharge of 45 mm/a that reaches values up to 140 mm/a in the most elevated areas (*Nisdafe* plateau) (CIAEH, 2018).

The geology of the *El Hierro* Island is typical of an oceanic island during the early stages of shield formation. Massive landslides have exposed the core structure of the island, which is constructed of two volcanic edifices that sequentially developed and collapsed: the *Tiñor* edifice (1.12–0.88 Ma) and the *El Golfo* edifice (545–175 ka) (García-Gil et al., 2023). Subsequently, these volcanic edifices were almost entirely covered by emissions from the rift volcanism (158 ka–present) (Fig. 1). The *Tiñor* edifice is restricted to the most northeastern subaerial part of the island. The *El Golfo* edifice was constructed as an attachment to the southwestern flank of the *Tiñor* edifice, and the rocks produced during this stage crop out on the escarpment of the *El Golfo* landslide. The rift volcanism features scoria cones and mafic lava flows emitted from eruptive fissures along the three-armed rift system that is responsible of the current island's morphology. During this stage, lava flows filled the space created by the *El Golfo* landslide (Volcanism of *El Golfo*).

Dykes trending parallel to the three axes of the rift system are a characteristic volcano-structural element on *El Hierro* Island. They are well exposed, with steeply dipping planes striking NE–SW, on the headwalls of the northern part of the *El Golfo* landslide, which cuts off them perpendicularly (Becerril et al., 2016, 2015). Dykes of *El Hierro* are predominantly mafic in composition and have a thickness ranging between 0.1 and 12.5 m. They are hosted by the alternating lava flows and pyroclastic layers of the *Tiñor* and *El Golfo* edifices. The relative younger Volcanism of *El Golfo* materials are not affected by dykes. Many dykes show glassy selvages and cooled edges at the contact with the host rock and ten of them were identified as feeder dykes or dykes directly connected to their eruptive fissures (Becerril et al., 2015, 2013).

Although precise hydraulic conductivity estimations are scarce, it is known that the rocks of the *El Golfo* edifice and Volcanism of *El Golfo* have a relative higher hydraulic conductivity than those of the *Tiñor* edifice because they are less compacted and altered, constituting the main aquifers of the island (IGME, 1997c). These geologic units act primarily as an island-scale unconfined aquifer, although there may be confined zones and local perched aquifers. By contrast, dykes have a much lower relative permeability than the hosting rocks, which has been confirmed by numerous wells and galleries drilled on the island for extracting drinking water (IGME, 1997c; Izquierdo, 2014; Santamarta, 2017). The majority of the wells and galleries are located in the *El Golfo* landslide area (Volcanism of *El Golfo* or *El Golfo* edifice materials), and most of them have been abandoned due to salinization by seawater intrusion (Ecker, 1976).

2.2. "Los Padrones" well-gallery description

The *Los Padrones* well-gallery is one of the few wells that is currently not affected by seawater intrusion (this was not always the case, as is explained later), despite being a shorter distance from the coastline than other wells (Fig. 1). The current *Los Padrones* well-gallery provides 1.20

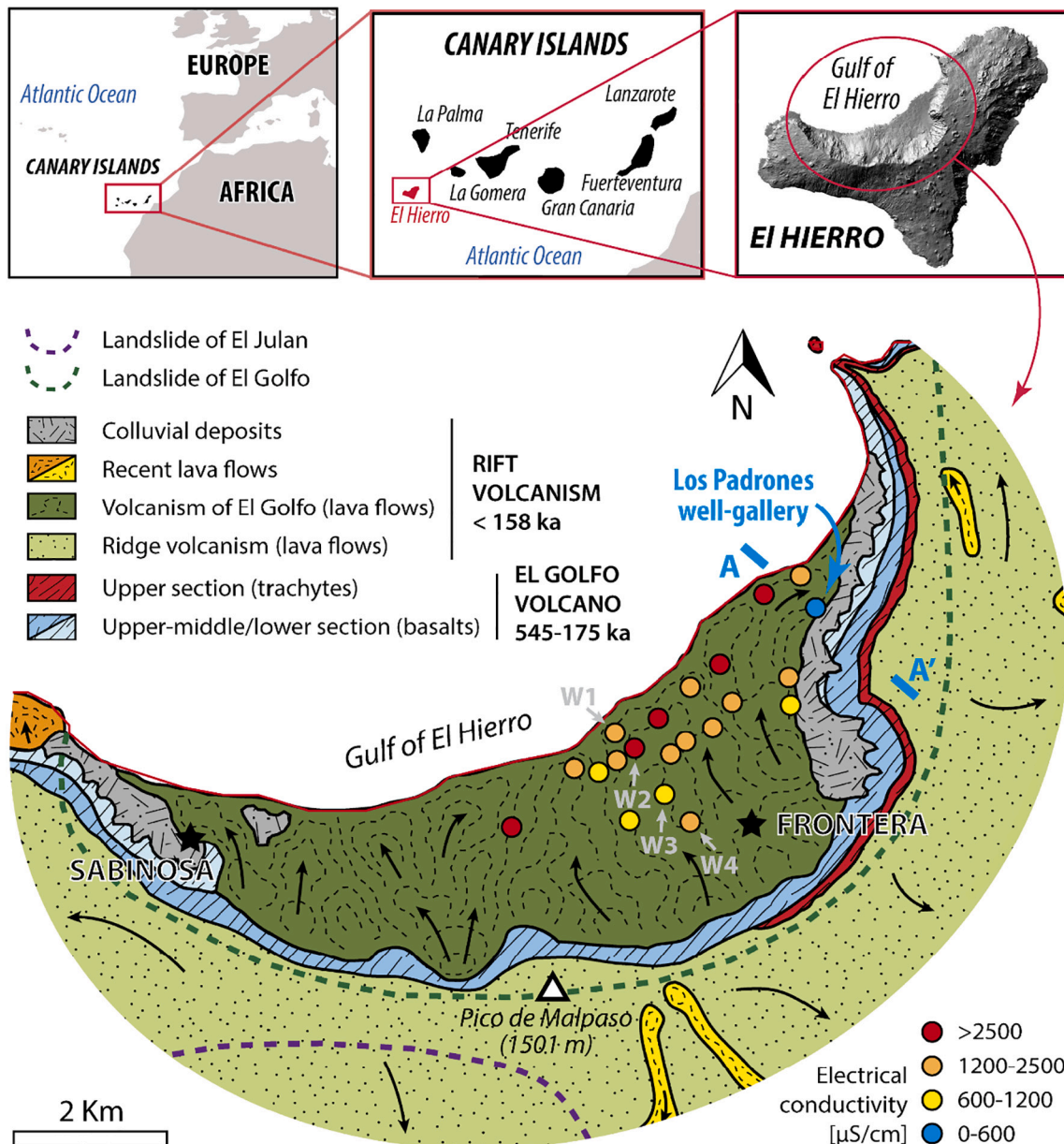


Fig. 1. Location and geological setting (García-Gil et al., 2023) of the study area on the *El Hierro* Island (Canary Islands, Spain). Note that electrical conductivity values measured in 2021 are shown in colour scale.

hm³/a of freshwater, which represents 52 % of the total water extracted from the aquifer by wells (2.30 hm³/a) and 37 % of the total annual water demand (3.28 hm³/a including urban, agriculture, livestock and industry demand) on the *El Hierro* Island (CIAEH, 2018). This extraction flow also represents 10 % of the total recharge of the island's aquifers and 32 % of the aquifer recharge feeding the *El Golfo* landslide area.

This critical hydraulic infrastructure for the supply of water on the island is composed of a vertical well 52 m long that connects at its bottom with a horizontal gallery (2 ‰ slope), a 2 × 2.5 m section that is 1011 m long that penetrates into the *Nisdafe* Plateau following a NW-SE direction (Figs. 2 and 3) (IGME, 2023; Navarro-Latorre, 1997; Servando-Molowny, 1998). The vertical well and the first 195 m of the horizontal gallery are drilled into the *Volcanism of El Golfo* materials, mainly constituted by compact olivine basalts of low permeability. From the discordance at 195 m onwards, the gallery crosses the materials of the *El Golfo* edifice with alternation of compact basalts, pyroclasts and volcanic slag of moderate permeability. On its way through the *El Golfo* edifice materials, the gallery crosses 40 dykes with a thickness ranging

between 0.1 and 6 m. Concrete closures and metal gates were constructed at the four thickest dykes, which were located at 200 (dyke 1, gate 1), 450 (dyke 11, gate 2), 650 (dyke 18, gate 3) and 1010 m (dyke 40, gate 4), in order to maintain original hydraulic heads and allow controlled water extraction by gravity from each interval (Fig. 3). At the end of the gallery (1011 m) there is a horizontal well that allows groundwater extraction beyond gate 4. The current horizontal gallery of 1011 m is the result of redrilling carried out in 1996 over the original horizontal gallery of 260 m. This redrilling was performed because, as occurred in most of the wells on the island (Ecker, 1976), when desired well yields were sustained over time, well water was salinized by seawater intrusion.

2.3. Hydrogeological and hydrochemical data

Hydraulic heads were measured in each interval between gates along the *Los Padrones* well-gallery and in four selected wells (W1 to W4) along a profile perpendicular to the coastline that crosses the *Volcanism of El*

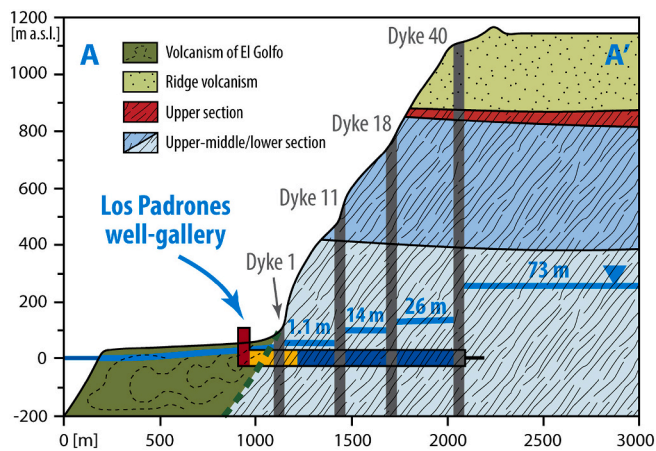


Fig. 2. Geological profile along the *Los Padrones* well-gallery (see its location in Fig. 1). The 3 parts of the *Los Padrones* well-gallery are shown: well (red), short gallery (yellow) and long gallery (blue). Note that the water table is not scaled vertically to improve visualization, but measured hydraulic head values are shown in blue lettering for each dyke interval.

Golfo materials in April 2021 (Fig. 1). The Ghyben-Herzberg analytical solution (Post et al., 2018b) was used to estimate the depth of the saline interface from measured hydraulic heads, assuming a density of 1000 kg/m³ for freshwater and 1027 kg/m³ for seawater.

Electrical conductivities were measured in April 2021 for the wells shown in Fig. 1. In addition, we analyzed major cations and anions of 274 samples along the *Los Padrones* well-gallery from 1998 to 2022 that were complemented with 3 sample analyses before and 10 after the redrilling carried out in 1996 (IGME, 2023).

2.4. Numerical model

A 2D synthetic density-driven groundwater flow and mass transport model was built with the FEFLOW code (Diersch, 2014) (Fig. 4), based on a hypothetical vertical profile along the *Los Padrones* well-gallery from the sea to the watershed (see the location of the profile in Fig. 1). The main geometric, hydraulic and mass transport characteristics of the model are summarized in Table 1 and are based on field data and literature (Poncela et al., 2022). The model domain had a length of 2500 m and a height that gradually ranged from 2000 m to 2300 m. This small variation in height did not have a large impact on transmissivity and prevented the top boundary condition from conditioning the results along the horizontal gallery, especially when extraction was activated. The horizontal gallery was placed at sea level, maintaining the real position with respect to the four main dykes that are evaluated in the model. The system was recharged on top with a constant rate of 100 mm/a and a salt concentration of 0 mg/l, which was normalized to the proportion of seawater (0 % seawater). A boundary condition representing sea level with a normalized concentration of 100 mg/l (100 % seawater) was set along the left side of the domain. The density ratio between the freshwater (1000 kg/m³) that recharged the top of the domain and the seawater (1027 kg/m³) that entered through the left boundary was set at 0.027. The right (watershed) and bottom boundaries were considered impermeable for flow and mass transport. The model did not attempt to calibrate specific investigation site conditions but used it as a basis for analysis of the impact of dykes on the geometry of the saline interface and, subsequently, on the availability of fresh groundwater resources. Thus, the flow perpendicular to the modeled profile was neglected.

The model was used to simulate 66 scenarios that resulted from assessing 6 different hydraulic conductivities for the dykes and 5 different extraction rates from 2 different strategic locations. The dykes hosted by a moderate hydraulic conductivity domain of 5 m/d were assessed with hydraulic conductivities of 5 (homogeneous; no dykes), 1,

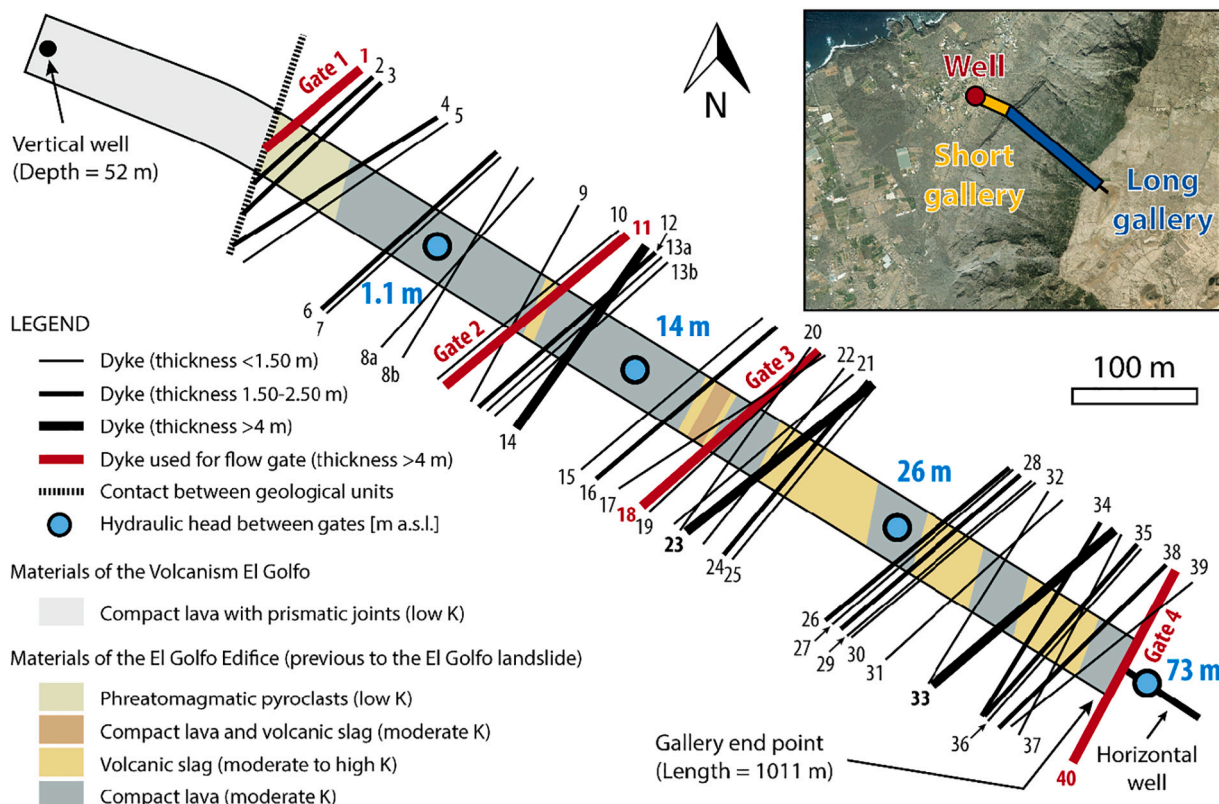


Fig. 3. Plan view and detailed geological mapping of the *Los Padrones* well-gallery (based on IGME, 2023; Navarro-Latorre, 1997; Servando-Molowny, 1998).

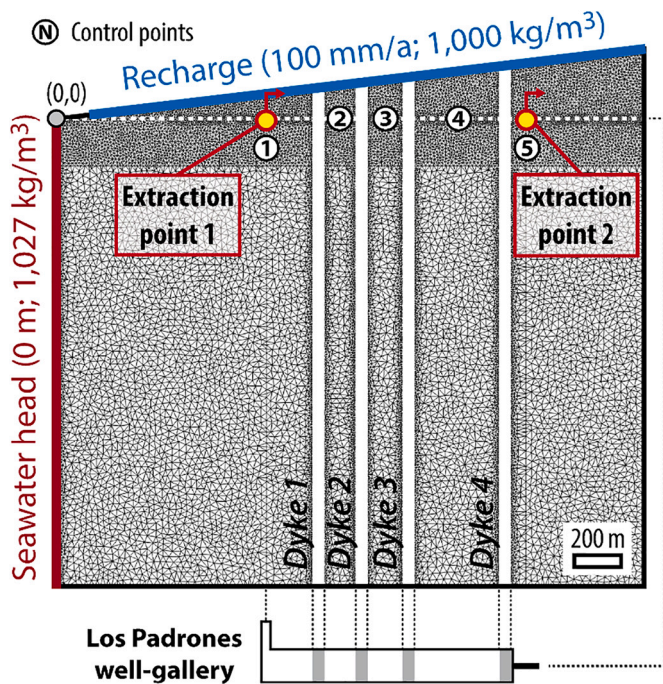


Fig. 4. Mesh and boundary conditions used for the density-driven groundwater flow model. Circled numbers show the measurement point (control points) for each of the five dyke intervals. The two extraction points assessed by modeling are indicated with yellow circles and coincide with control points 1 and 5.

Table 1
Summary table of mesh, time and hydraulic and mass transport parameters used in the numerical model.

Parameter	Value	Units
Mesh and time parameters		
Problem projection	Vertical confined 2D aquifer	[-]
Minimum height (Y axis)	2000	[m]
Maximum height (Y axis)	2300	[m]
Length (X axis)	2500	[m]
Mesh elements	41,835	[-]
Simulation time	∞ (quasi-stationary)	[-]
Hydraulic parameters		
Hydraulic conductivity	5	[m/d]
Hydraulic conductivity (dykes)	5 (homogeneous); 1; 0.1; 0.01; 0.001; 0.0001	[m/d]
Density ratio	0.027	[-]
Recharge (top)	100	[mm/a]
Seawater head BC (left side)	0	[m]
Extraction rate (% of recharge)	10; 20; 30; 40; 50	[%]
Mass transport parameters		
Longitudinal dispersivity	10	[m]
Transversal dispersivity	1	[m]
Porosity	0.1	[%]
Mass-concentration (top)	0 (normalized to 0 % of seawater)	[mg/l]
Mass-concentration (left side)	100 (normalized to 100 % of seawater)	[mg/l]

0.1, 0.01, 0.001 and 0.0001 m/d. In addition, from each of these scenario results, we evaluated what happens if 10, 20, 30, 40 and 50 % of the recharged water in the system was extracted from the starting point (extraction point 1 in Fig. 4, where vertical well intersects the horizontal gallery) and the ending point (extraction point 2 in Fig. 4) of the horizontal gallery. All the simulations were run until reaching a quasi-stationary state, where hydraulic parameters such as porosity no longer influenced results.

3. Results and discussion

3.1. Dykes condition the quantity and quality of groundwater on El Hierro Island

Hydraulic heads and salinity proxies measured along the *Los Padrones* gallery confirmed the impact of dykes on the availability of fresh groundwater on *El Hierro* Island. The detailed geological mapping carried out in the *Los Padrones* gallery (Fig. 3) demonstrated the existence of 40 dykes between meters 195 and 1011 of the gallery (*El Golfo* edifice materials). The presence of a swarm of sub-vertical dykes parallel to the coast compartmentalized the aquifer of the *El Golfo* edifice materials, giving rise to a stepped water table with a hydraulic gradient more than ten times greater than in the adjacent aquifer of the volcanism *El Golfo* materials (Fig. 5A). Each dyke generated an impact of different magnitude on the system, depending on its inclination, direction and, especially, thickness. Four of the thickest dykes (dykes 1, 11, 18 and 40, Figs. 2 and 3) generated the greatest staggering on the water table during the drilling, rising to 1.1 m a.s.l. after dyke 1, to 14 m a.s.l. after dyke 11, to 26 m a.s.l. after dyke 18 and finally to 73 m a.s.l. after dyke 40. The rest of the dykes caused a minor or negligible impact on the water table. These field data demonstrated the need to analyze dyke swarms at the local scale, since the expected behavior of each dyke can be very different even when they have a similar apparent thickness in

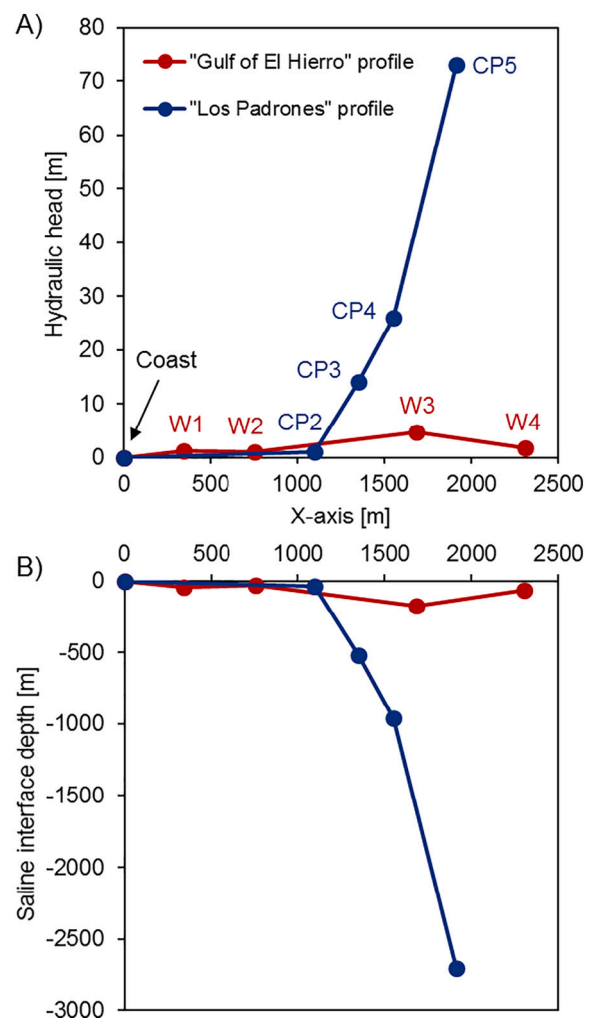


Fig. 5. A) Measured hydraulic heads along the Gulf of *El Hierro* (see the location of wells, W, in Fig. 1) and *Los Padrones* profiles (see the location of control points, CP, in Fig. 4). B) Calculated depth of the saline interface along both profiles using the Ghyben-Herzberg analytical solution.

the mapped area.

The concentration of chlorine and the electrical conductivity measured in the water extracted from the vertical well, or beginning of the *Los Padrones* gallery, from the short gallery that was initially drilled (in operation until 1996) and from the end of the current gallery of 1011 m, demonstrated the impact of the dykes on water quality (Fig. 6). The average electrical conductivity in the well decreased from 1450 $\mu\text{S}/\text{cm}$ to 420 $\mu\text{S}/\text{cm}$ when the short gallery was dug, which meant going from water strongly affected by seawater intrusion to drinking water. This sharp change occurred, shifting the extraction point 260 m (the length of the short gallery) from the original well drilled into the Volcanism of *El Golfo* materials (not affected by dykes) to the new emplacement into the *El Golfo* edifice materials (affected by dykes). In addition, the end of the short gallery was at a distance from the coast where the wells located in the Gulf of *El Hierro* (Volcanism of *El Golfo*) were strongly affected by seawater intrusion (Fig. 1), especially when subjected to intensive pumping. This abrupt change in salinity and the difference to what was observed in the Gulf of *El Hierro* can only be explained by the fact that the saline interface was deeper in the materials affected by dykes (*El Golfo* edifice) than in the materials that fill the gulf and are not affected by dykes (Volcanism of *El Golfo*). The average electrical conductivity dropped to 350 $\mu\text{S}/\text{cm}$ when the gallery was lengthened up to the current length of 1011 m, allowing intensive extraction of 1.20 hm^3/a (37 % of the total annual water demand of the island) without increasing water salinity. This presumed an anomaly on the island where most of the wells got salinized and confirmed that the saline interface in the aquifer affected by dykes (*El Golfo* edifice) was deeper. Also the depths of the saline interface calculated by the Ghyben-Herzberg analytical solution from measured hydraulic heads confirmed this hypothesis (Fig. 5B), which will be assessed numerically in the next section.

3.2. Impact of dykes on the depth of the saline interface

Numerical assessment of the impact of dykes on the geometry of the saline interface in coastal and island aquifers confirmed that the presence of these low-permeability volcanic structures leads to a deeper saline interface on the inland side than on the seaward side. The six density-driven flow simulations carried out, with a synthetic model based on the *Los Padrones* profile, calculated a progressive increase in the depth and thickness of the saline interface as the hydraulic conductivity of the dykes decreased (Figs. 7 and 8A).

Taking as reference sea level and the surface that represents the 50 %

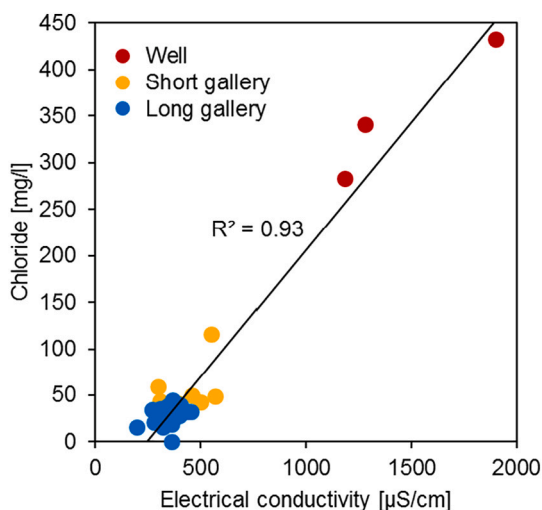


Fig. 6. Relationship between electrical conductivity and chloride for groundwater samples extracted at different stretches of the *Los Padrones* well-gallery. Note the progressive reduction in the degree of salinization from the vertical well to the end of the long gallery after 40 dykes.

mixture between fresh and sea water, the depth of the saline interface at control point 5 (the interval between dykes furthest from the sea; see its location in Fig. 4) increased drastically from 80 m (Fig. 7A), when the whole domain was considered homogeneous without dykes, to 2000 m, when dykes were activated with $K_d = 0.0001 \text{ m/d}$ (Fig. 7F). The greater depth of the saline interface on the inland side of the dyke compared to the seaward side implied that fresh groundwater reserves were also increased inland as a consequence of the effect of low-permeability dykes. In addition, the presence of several dykes produced a cumulative effect from the sea to inland (Fig. 8A). When low-permeability dykes were activated, the depth of the saline interface tended to decrease between the coastline and the first dyke, which implied a greater probability of salinization for the wells located in that area (Figs. 7 and 8A). The thickness of the saline interface also increased as the hydraulic conductivity of the dykes decreased.

The impact of low-permeability dykes on the geometry of the saline interface was explained by the staggering and relative increase that occurred in the water table. Since the saline interface represented the hydrostatic equilibrium between the relative less dense fresh groundwater and the relative more dense seawater, the relative higher hydraulic heads associated with the staggering of the water table led to a deepening of the saline interface. In the case of *El Hierro* Island, as previously discussed, the hydraulic gradient along the *Los Padrones* profile (affected by dykes), was much larger than along the Gulf of *El Hierro* profile (Fig. 5A). For this reason, the saline interface was much deeper in the materials affected by dykes (*El Golfo* edifice) than in the materials that fill the Gulf of *El Hierro* (Volcanism of *El Golfo*) (Fig. 5B). In the absence of dykes, the low recharge rate by rain infiltration, together with the limited dimensions of islands, lead to a water table with very low hydraulic gradients and, subsequently, to a very shallow saline interface that favors salinization of wells. This explained why most of the wells in the Gulf of *El Hierro* (Fig. 1), and probably in other islands globally, have been abandoned due to salinization (Custodio et al., 2016; Ecker, 1976; Izuka et al., 2018).

Even though the objective of the 2D numerical model was not to calibrate the local conditions of the *Los Padrones* site, the trend in the staggering of measured hydraulic heads was very similar to those calculated by the model when the dykes were activated with a K_d between 0.001 and 0.0001 m/d (Figs. 7E and F and 8B). This confirmed the impermeable effect of dykes on *El Hierro* Island and can serve as a basis for future research on the island. In addition, the simulation that considered a homogenous domain without dykes (Fig. 7A) also provided a good approximation of the expected geometry of the saline interface along the Gulf of *El Hierro* profile.

3.3. Dykes are critical for the production of drinking water in coastal and island aquifers

The impact of low-permeability dykes on the geometry and, subsequently, on the depth of the saline interface was demonstrated to be critical in assessing fresh groundwater resources and in deciding on the location of drinking water production wells, in order to ensure the best possible water quality. The 66 simulations carried out to evaluate the effect of dykes on the salinity of extracted water showed that wells located inland from dykes allowed a fresh groundwater extraction rate that is much higher than wells located seaward from dykes, without becoming salinized (Fig. 9).

The extracted water was affected by seawater intrusion in all scenarios when water extraction was carried out from extraction point 1, which was located between the coastline and the first dyke (see the exact location in Fig. 4) (Fig. 9A). Extraction point 1 became salinized even when there was no extraction. The mixing ratio of seawater increased as the hydraulic conductivity of dykes reduced, reaching >50 % of the extracted water when $K_d = 0.0001$. The proportion of seawater increased linearly, as did the extraction rate.

However, the presence of low-permeability dykes allowed extraction

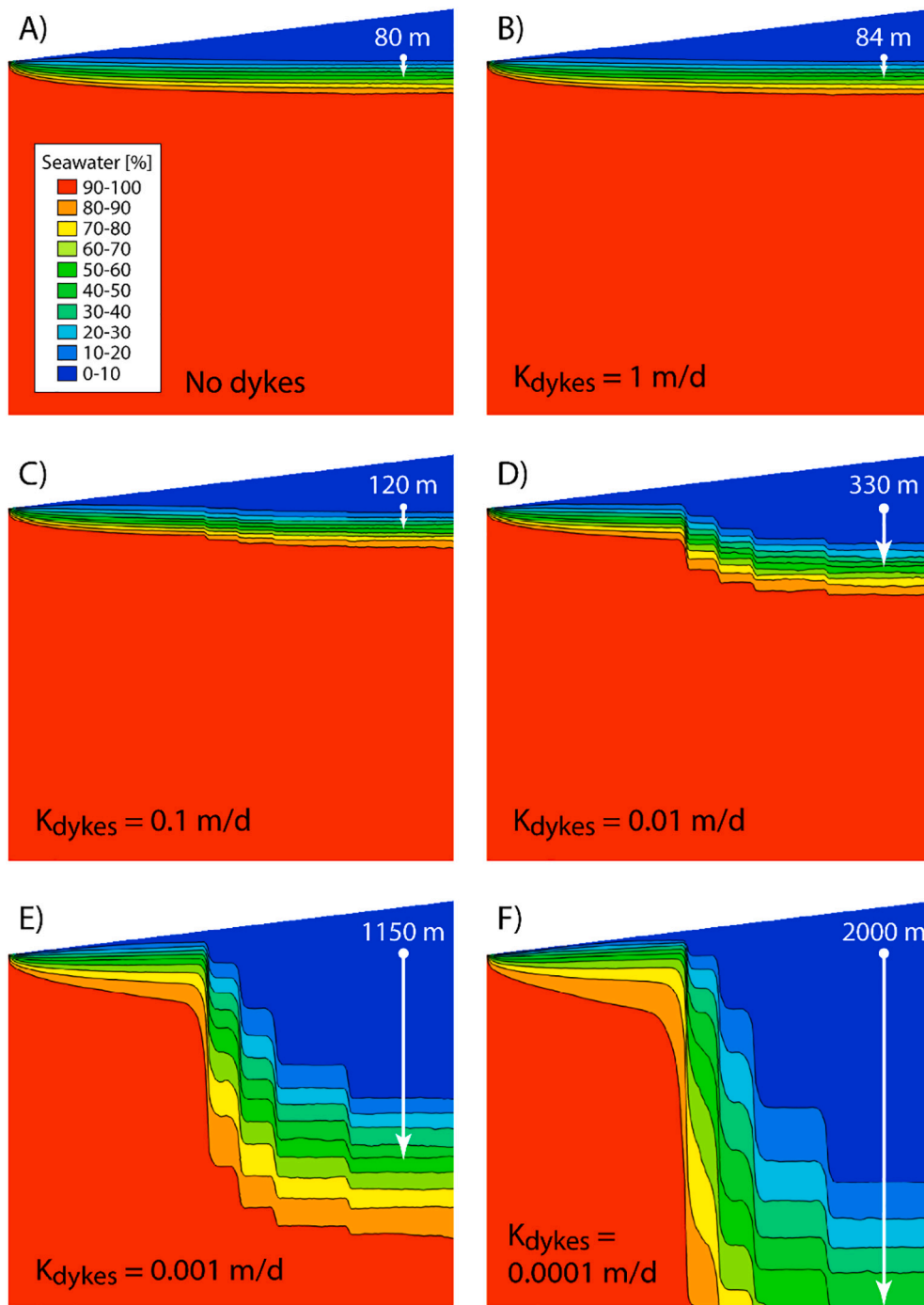


Fig. 7. Percentage of seawater calculated by the density-driven groundwater numerical model in each scenario. Note the progressive increase in the depth of the saline interface as the hydraulic conductivity of the dykes reduces from 5 m/d (homogeneous case) in A to 0.0001 m/d in F.

of pure freshwater from extraction point 2 (Fig. 9B). The relative deeper saline interface at this point, as a consequence of low-permeability dykes (simulations with $K_d = 0.001$ and 0.0001 m/d), ensured avoiding any seawater contribution when up to 20 % of the recharged water was extracted, or up to 30 % with a seawater contribution <1 %. For extraction flows >30 % of the recharged water, the model results showed mixing with seawater but always in a lower proportion than in the scenario that did not consider dykes.

Although studies and models considering the specific local hydrogeological characteristics are necessary, these results demonstrated that the presence of low-permeability dykes can prevent the abandonment of wells and galleries due to salinization in coastal areas, if they are

correctly located. Locations inland from the dykes were beneficial in avoiding the effect of saline intrusion on extraction wells, while locations closer to the coast may be detrimental. In addition, extraction flows can become as important as 20 % or 30 % of the water recharged in the aquifer, which is key for ensuring drinking water supply on islands.

4. Conclusions

In this paper, we evaluated the impact of volcanic dykes on the depth of the saline interface in coastal and island aquifers and, subsequently, on the availability of fresh groundwater. We integrated, for the first time, in situ hydraulic and hydrochemical data from a well-gallery that

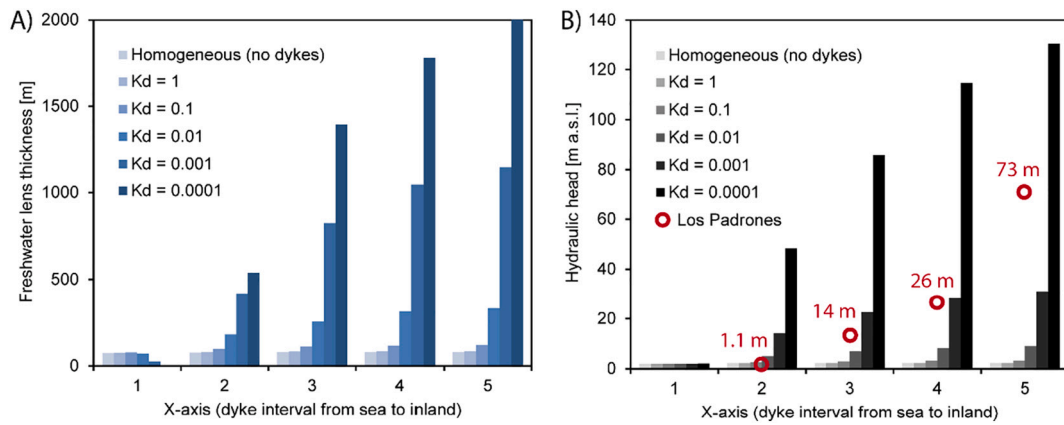


Fig. 8. A) Computed thickness of the freshwater lens at each dyke interval (see the locations of control points in Fig. 4) for the 6 simulated scenarios that assessed the impact of the hydraulic conductivity of dykes (K_d) on the freshwater lens geometry. B) Computed hydraulic head and measured hydraulic head in the *Los Padrones* well-gallery at each dyke interval.

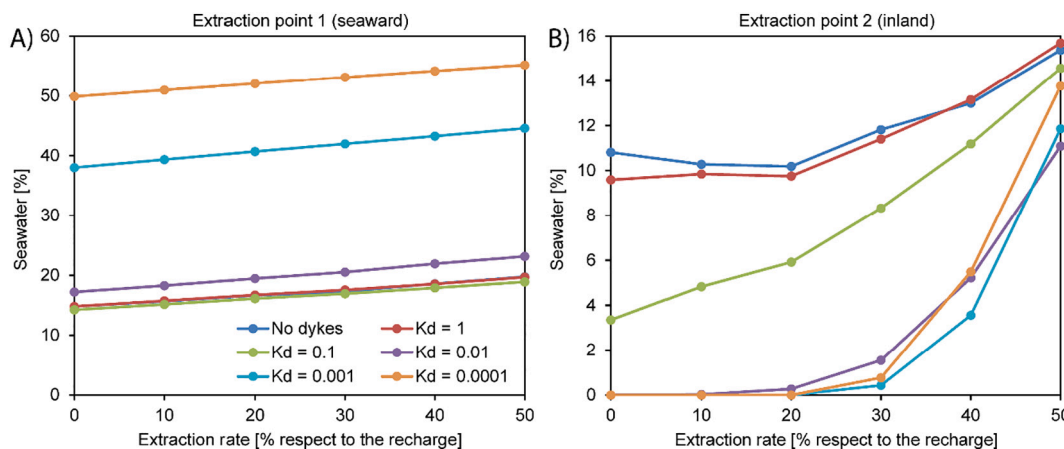


Fig. 9. Computed mixing ratio of seawater versus extraction rate (from 0 % to 50 % of the recharge) for the two assessed locations of the extraction point (at the beginning of the gallery or before dykes, A, and at the end of the gallery or after the dykes, B). See the exact locations of extraction points 1 and 2 in Fig. 4.

crosses 40 dykes perpendicularly along its >1000 m length on *El Hierro* Island (Canary Islands, Spain), along with numerical modeling. The *Los Padrones* well-gallery supplied 37 % of the water demand on the island, even though it was one of the few wells not affected by seawater intrusion, making it an outstanding case.

Measured hydraulic heads along the *Los Padrones* well-gallery demonstrated that the staggering of the water table was mainly controlled by a few dykes, the four thickest ones. In addition, the presence of dykes increased the hydraulic gradient more than one order of magnitude with respect to the adjacent aquifer, which is not affected by dykes. This stepwise increase in hydraulic heads pushed the saline interface downward and reduced electrical conductivity from 1450 $\mu\text{S}/\text{cm}$ to 350 $\mu\text{S}/\text{cm}$ along the gallery, which was a much lower value than those measured in the adjacent aquifer at the same distance from the coast.

Numerical assessment of the impact of dykes on the geometry of the saline interface confirmed that the lower the hydraulic conductivity of the dykes, the greater the depth of the saline interface inland. This impact of dykes on the geometry of the saline interface led to increasing fresh groundwater reserves inland, relative to a hypothetical case without dykes. However, the depth of the saline interface tended to decrease between the coastline and the first dyke, as the permeability of dykes decreased.

Numerical simulations also demonstrated that dykes can prevent the abandonment of drinking water production wells due to salinization in

coastal and island aquifers if they are correctly placed. Locating production wells far enough inland in an area affected by dykes allowed a higher freshwater extraction rate than if dykes did not exist, while near the coastline, the effect tended to be the opposite. In the case of the *Los Padrones* well-gallery, the drilling of a horizontal gallery from the original vertical well made it possible to go from extracting water with an electrical conductivity of 1450 $\mu\text{S}/\text{cm}$, not suitable for human consumption, to extracting high quality water of 350 $\mu\text{S}/\text{cm}$, with extraction rates that cover almost half of the island’s water demand.

These results will help improve the exploitation strategies of fresh groundwater resources in coastal volcanic aquifers, and especially on volcanic islands such as the Hawaiian Islands or the Macaronesian archipelagos. As a general rule, it is recommended to locate drinking water production wells in inland areas affected by dykes, since they are the most protected areas from saline intrusion and host the largest reserves of fresh groundwater in the case of islands. In addition, these results will serve as the basis for future 3D modeling approaches that analyze the impact of dykes on piezometry and hydrochemistry at the island aquifer scale.

CRediT authorship contribution statement

Miguel Ángel Marazuela: Conceptualization, Methodology, Investigation, Writing – original draft, Visualization, Formal analysis, Project administration. **Carlos Baquedano:** Writing – review & editing. **Noelia**

Cruz-Pérez: Writing – review & editing. **Jorge Martínez-León:** Writing – review & editing. **Chrysi Lapidou:** Funding acquisition. **Juan Carlos Santamarta:** Writing – review & editing, Project administration, Funding acquisition. **Alejandro García-Gil:** Writing – review & editing, Project administration, Funding acquisition.

Declaration of competing interest

The authors declare the following financial interests/personal relationships which may be considered as potential competing interests: Alejandro Garcia Gil reports financial support was provided by Government of Spain. Alejandro Garcia Gil reports financial support was provided by European Union.

Data availability

Data will be made available on request.

Acknowledgments

This research was supported by the European Union's Horizon 2020 Research and Innovation Program (ARSINOE project, 101037424), and the Spanish Research Agency (SAGE4CAN project, PID2020-114218RA-I00). The authors are grateful to the *Consejo Insular de Aguas de El Hierro* for the valuable support.

References

- Abarca, E., Carrera, J., Sánchez-Vila, X., Dentz, M., 2007. Anisotropic dispersive Henry problem. *Adv. Water Resour.* 30, 913–926. <https://doi.org/10.1016/j.advwatres.2006.08.005>.
- Bear, J., Cheng, A.H.-D., Sorek, S., Ouazar, D., Herrera, I., 1999. *Seawater Intrusion in Coastal Aquifers-Concepts, Methods and Practices*. Springer Dordrecht. <https://doi.org/10.1007/978-94-017-2969-7>.
- Becerril, L., Galindo, I., Gudmundsson, A., Morales, J.M., 2013. Depth of origin of magma in eruptions. *Sci. Rep.* 3, 1–6. <https://doi.org/10.1038/srep02762>.
- Becerril, L., Galindo, I., Martí, J., Gudmundsson, A., 2015. Three-armed rifts or masked radial pattern of eruptive fissures? The intriguing case of El Hierro volcano (Canary Islands). *Tectonophysics* 647, 33–47. <https://doi.org/10.1016/j.tecto.2015.02.006>.
- Becerril, L., Galve, J.P., Morales, J.M., Romero, C., Sánchez, N., Martí, J., Galindo, I., 2016. Volcano-structure of El Hierro (Canary Islands). *J. Maps* 12, 43–52. <https://doi.org/10.1080/17445647.2016.1157767>.
- Bedekar, V.S., Memari, S.S., Clement, T.P., 2019. Investigation of transient freshwater storage in island aquifers. *J. Contam. Hydrol.* 221, 98–107. <https://doi.org/10.1016/j.jconhyd.2019.02.004>.
- Cao, T., Han, D., Song, X., 2021. Past, present, and future of global seawater intrusion research: a bibliometric analysis. *J. Hydrol.* 603, 126844. <https://doi.org/10.1016/j.jhydrol.2021.126844>.
- Chang, Q., Zheng, T., Chen, Y., Zheng, X., Walther, M., 2020. Investigation of the elevation of saltwater wedge due to subsurface dams. *Hydrol. Process.* 34, 4251–4261. <https://doi.org/10.1002/hyp.13863>.
- CIAEH, 2018. *Hydrological Plan of El Hierro (2015–2021)*.
- Comte, J.C., Wilson, C., Ofterdinger, U., González-Quirós, A., 2017. Effect of volcanic dykes on coastal groundwater flow and saltwater intrusion: a field-scale multiphysics approach and parameter evaluation. *Water Resour. Res.* 53, 2171–2198. <https://doi.org/10.1002/2016WR019480>.
- Custodio, E., 2007. Groundwater in volcanic hard rocks. In: Krásný, J., Sharp, J.M. (Eds.), *Groundwater in Fractured Rocks*. CRC Press, p. 14. <https://doi.org/10.1201/9780203945650.ch5>.
- Custodio, E., Cabrera, M. del C., Poncela, R., Puga, L.O., Skupien, E., del Villar, A., 2016. Groundwater intensive exploitation and mining in Gran Canaria and Tenerife, Canary Islands, Spain: hydrogeological, environmental, economic and social aspects. *Sci. Total Environ.* 557–558, 425–437. <https://doi.org/10.1016/j.scitotenv.2016.03.038>.
- Diersch, H.-J.G., 2014. *FEFLOW: Finite Element Modeling of Flow, Mass and Heat Transport in Porous and Fractured Media*. Springer-Verlag, Berlin Heidelberg. <https://doi.org/10.1007/978-3-642-38739-5>.
- Ecker, A., 1976. Groundwater behavior in Tenerife, Volcanic Island (Canary Islands, Spain). *J. Hydrol.* 28, 73–86. [https://doi.org/10.1016/0022-1694\(76\)90053-6](https://doi.org/10.1016/0022-1694(76)90053-6).
- Etsias, G., Hamill, G.A., Campbell, D., Straney, R., Benner, E.M., Águila, J.F., McDonnell, M.C., Ahmed, A.A., Flynn, R., 2021. Laboratory and numerical investigation of saline intrusion in fractured coastal aquifers. *Adv. Water Resour.* 149, 103866. <https://doi.org/10.1016/j.advwatres.2021.103866>.
- Fernandes, A.L., Cruz, J.V., Figueira, C., Prada, S., 2020. Groundwater chemistry in Madeira Island (Portugal): main processes and contribution to the hydrogeological conceptual model. *Environ. Earth Sci.* 79, 1–19. <https://doi.org/10.1007/s12665-020-09151-8>.
- Fetter Jr., C.W., 1972. Position of the saline water interface beneath oceanic islands. *Water Resour. Res.* 8, 1307–1315. <https://doi.org/10.1029/WR008i005p01307>.
- Folch, A., del Val, L., Luquot, L., Martínez-Pérez, L., Bellmunt, F., Le Lay, H., Rodellas, V., Ferrer, N., Palacios, A., Fernández, S., Marazuela, M.A., Diego-Feliu, M., Pool, M., Goyetche, T., Ledo, J., Pezard, P., Bour, O., Queralt, P., Marcuello, A., García-Orellana, J., Saaltink, M.W., Vázquez-Suñé, E., Carrera, J., 2020. Combining fiber optic DTS, cross-hole ERT and time-lapse induction logging to characterize and monitor a coastal aquifer. *J. Hydrol.* 588, 125050. <https://doi.org/10.1016/j.jhydrol.2020.125050>.
- Font-Capó, J., Vázquez-Suñé, E., Carrera, J., Martí, D., Carbonell, R., Pérez-Estaun, A., 2011. Groundwater inflow prediction in urban tunneling with a tunnel boring machine (TBM). *Eng. Geol.* 121, 46–54. <https://doi.org/10.1016/j.enggeo.2011.04.012>.
- Font-Capó, J., Vázquez-Suñé, E., Carrera, J., Herms, I., 2012. Groundwater characterization of a heterogeneous granitic rock mass for shallow tunneling. *Geol. Acta* 10, 395–408. <https://doi.org/10.1344/105.000001773>.
- García-Gil, A., Poncela Poncela, R., Skupien Balon, E., Morales González-Moro, Á., Lario-Báscones, R.J., Marazuela, M.Á., Cruz-Pérez, N., Santamarta, J.C., 2022. Heterogeneity-driven hydrodynamics conditions the hydrochemistry of spring water in Volcanic Islands. *Groundwater* 61, 375–388. <https://doi.org/10.1111/gwat.13249>.
- García-Gil, A., Baquedano, C., Marazuela, M.Á., Martínez-León, J., Cruz-Pérez, N., Hernández-Gutiérrez, L.E., Santamarta, J.C., 2023. A 3D geological model of El Hierro volcanic island reflecting intraplate volcanism cycles. *Groundw. Sustain. Dev.* 21, 100936. <https://doi.org/10.1016/j.gsd.2023.100936>.
- Geng, X., Michael, H.A., 2020. Preferential flow enhances pumping-induced saltwater intrusion in volcanic aquifers. *Water Resour. Res.* 56, 1–15. <https://doi.org/10.1029/2019WR026390>.
- Giese, M., Barthel, R., 2021. Review: saltwater intrusion in fractured crystalline bedrock. *Hydrogeol. J.* 29, 2313–2328. <https://doi.org/10.1007/s10040-021-02396-y>.
- Glover, R.E., 1959. The pattern of fresh-water flow in a coastal aquifer. *J. Geophys. Res.* 64, 457–459. <https://doi.org/10.1029/jz064i004p00457>.
- Hernández Ríos, I., Cruz-Pérez, N., Chirivella-Guerra, J.I., García-Gil, A., Rodríguez-Alcántara, J.S., Rodríguez-Martín, J., Marazuela, M.Á., Santamarta, J.C., 2023. Proposed recharge of island aquifer by deep wells with regenerated water in Gran Canaria (Spain). *Groundw. Sustain. Dev.* 22, 100959. <https://doi.org/10.1016/j.gsd.2023.100959>.
- Houben, G., Post, V.E.A., 2017. The first field-based descriptions of pumping-induced saltwater intrusion and upconing. *Hydrogeol. J.* 25, 243–247. <https://doi.org/10.1007/s10040-016-1476-x>.
- Houben, G.J., Stoeckl, L., Mariner, K.E., Choudhury, A.S., 2018. The influence of heterogeneity on coastal groundwater flow - physical and numerical modeling of fringing reefs, dykes and structured conductivity fields. *Adv. Water Resour.* 113, 155–166. <https://doi.org/10.1016/j.advwatres.2017.11.024>.
- IGME, 1997a. *Sheet and Report N° 1105-II Isla de El Hierro - Valverde (Madrid)*.
- IGME, 1997b. *Sheet and Report N° 1105-III Isla de El Hierro - Sabinosa (Madrid)*.
- IGME, 1997c. *Sheet and Report N° 1105-IV Isla de El Hierro - Frontera (Madrid)*.
- IGME, 1997d. *Sheet and Report N° 1105-II/I Isla de El Hierro - La Restinga (Madrid)*.
- IGME, 2023. *Dataset Catalog of the Geological and Mining Institute of Spain*.
- Izquierdo, T., 2014. Conceptual hydrogeological model and aquifer system classification of a small volcanic island (La Gomera; Canary Islands). *Catena* 114, 119–128. <https://doi.org/10.1016/j.catena.2013.11.006>.
- Izuka, S.K., Gingerich, S.B., 1998. Estimation of the depth to the fresh-water/salt-water interface from vertical head gradients in wells in coastal and island aquifers. *Hydrogeol. J.* 6, 365–373. <https://doi.org/10.1007/s100400050159>.
- Izuka, S., Engott, J.A., Rotzoll, K., Bassiouni, M., Johnson, A.G., Miller, L.D., Mair, A., 2018. *Volcanic Aquifers of Hawaii-i-Hydrogeology, Water Budgets, and Conceptual Models (ver. 2.0, March 2018)*. <https://doi.org/10.3133/sir20155164>.
- Kreyns, P., Geng, X., Michael, H.A., 2020. The influence of connected heterogeneity on groundwater flow and salinity distributions in coastal volcanic aquifers. *J. Hydrol.* 586, 124863. <https://doi.org/10.1016/j.jhydrol.2020.124863>.
- Lachassagne, P., Aunay, B., Frissant, N., Guilbert, M., Malard, A., 2014. High-resolution conceptual hydrogeological model of complex basaltic volcanic islands: a Mayotte, Comoros, case study. *Terra Nov.* 26, 307–321. <https://doi.org/10.1111/ter.12102>.
- Leoni, B., Zanotti, C., Nava, V., Rotiroli, M., Stefania, G.A., Fallati, L., Soler, V., Fumagalli, L., Savini, A., Galli, P., Bonomi, T., 2021. Freshwater system of coral inhabited island: availability and vulnerability (Magoodhoo Island of Faafu Atoll – Maldives). *Sci. Total Environ.* 785, 147313. <https://doi.org/10.1016/j.scitotenv.2021.147313>.
- Lopes, D., Barbosa, S., Cruz-Pérez, N., García-Gil, A., Marazuela, M.Á., Rodríguez-Alcántara, J.S., Santamarta, J.C., 2022. Excess of naturally occurring fluoride in groundwater discharge in Macaronesia: Brava Island, Cape Verde. *Water* 14, 3421. <https://doi.org/10.3390/w14213421>.
- Mahmoodzadeh, D., Karamouz, M., 2019. Seawater intrusion in heterogeneous coastal aquifers under flooding events. *J. Hydrol.* 568, 1118–1130. <https://doi.org/10.1016/j.jhydrol.2018.11.012>.
- Marazuela, M.A., Vázquez-Suñé, E., Custodio, E., Palma, T., García-Gil, A., Ayora, C., 2018. 3D mapping, hydrodynamics and modelling of the freshwater-brine mixing zone in salt flats similar to the Salar de Atacama (Chile). *J. Hydrol.* 561, 223–235. <https://doi.org/10.1016/j.jhydrol.2018.04.010>.
- Marazuela, M.A., Ayora, C., Vázquez-Suñé, E., Olivella, S., García-Gil, A., 2020. Hydrogeological constraints for the genesis of the extreme lithium enrichment in the Salar de Atacama (NE Chile): a thermohaline flow modelling approach. *Sci. Total Environ.* 739, 139959. <https://doi.org/10.1016/j.scitotenv.2020.139959>.
- Marazuela, M.Á., García-Gil, A., Santamarta, J.C., Gasco-Cavero, S., Cruz-Pérez, N., Hofmann, T., 2022. Stormwater management in urban areas using dry gallery

- infiltration systems. *Sci. Total Environ.* 823, 153705 <https://doi.org/10.1016/j.scitotenv.2022.153705>.
- Martínez-Pérez, L., Luquot, L., Carrera, J., Marazuela, M.A., Goyetche, T., Pool, M., Palacios, A., Bellmunt, F., Ledo, J., Ferrer, N., del Val, L., Pezard, P.A., García-Orellana, J., Diego-Feliu, M., Rodellas, V., Saaltink, M.W., Vázquez-Suné, E., Folch, A., 2022. A multidisciplinary approach to characterizing coastal alluvial aquifers to improve understanding of seawater intrusion and submarine groundwater discharge. *J. Hydrol.* 607, 127510 <https://doi.org/10.1016/j.jhydrol.2022.127510>.
- Mualem, Y., Bear, J., 1974. The shape of the interface in steady flow in a stratified aquifer. *Water Resour. Res.* 10, 1207–1215. <https://doi.org/10.1029/WR010i006p01207>.
- Navarro-Latorre, J.M., 1997. Levantamiento geológico de la galería del pozo de Los Padrones.
- Parizi, E., Hosseini, S.M., Ataie-Ashtiani, B., Simmons, C.T., 2019. Vulnerability mapping of coastal aquifers to seawater intrusion: review, development and application. *J. Hydrol.* 570, 555–573. <https://doi.org/10.1016/j.jhydrol.2018.12.021>.
- Perrin, J., Ahmed, S., Hunkeler, D., 2011. The effects of geological heterogeneities and piezometric fluctuations on groundwater flow and chemistry in a hard-rock aquifer, southern India. *Hydrogeol. J.* 19, 1189–1201. <https://doi.org/10.1007/s10040-011-0745-y>.
- Poncela, R., Santamarta, J.C., García-Gil, A., Cruz-Pérez, N., Skupien, E., García-Barba, J., 2022. Hydrogeological characterization of heterogeneous volcanic aquifers in the Canary Islands using recession analysis of deep water gallery discharge. *J. Hydrol.* 610, 127975 <https://doi.org/10.1016/j.jhydrol.2022.127975>.
- Post, V.E.A., Bosserelle, A.L., Galvis, S.C., Sinclair, P.J., Werner, A.D., 2018a. On the resilience of small-island freshwater lenses: evidence of the long-term impacts of groundwater abstraction on Bonriki Island, Kiribati. *J. Hydrol.* 564, 133–148. <https://doi.org/10.1016/j.jhydrol.2018.06.015>.
- Post, V.E.A., Houben, G.J., van Engelen, J., 2018b. What is the Ghijben-Herzberg principle and who formulated it? *Hydrogeol. J.* 26, 1801–1807. <https://doi.org/10.1007/s10040-018-1796-0>.
- Post, V.E.A., Galvis, S.C., Sinclair, P.J., Werner, A.D., 2019. Evaluation of management scenarios for potable water supply using script-based numerical groundwater models of a freshwater lens. *J. Hydrol.* 571, 843–855. <https://doi.org/10.1016/j.jhydrol.2019.02.024>.
- Santamarta, J.C., 2017. Tratado de minería de recursos hídricos en islas volcánicas oceánicas. Colegio Oficial de Ingenieros de Minas del Sur de España, Colegio Oficial de Ingenieros de Minas del Sur.
- Santamarta, J.C., Hernández-Sánchez, C., 2007. La isla de El Hierro (archipiélago canario, España); solución a la intrusión marina y futuro de la gestión hidráulica de la isla. In: Pulido Bosch, A., López-Geta, J.A., Ramos González, G. (Eds.), *Los Acuíferos Costeros: Retos y Soluciones, Coastal Aquifers: Challenges and Solutions*. Geological and Mining Institute of Spain, pp. 1085–1095.
- Santamarta, J.C., Rodríguez-Martín, J., 2020. Los procesos de planificación hidrológica en la península ibérica e islas en un contexto de cambio climático. Colegio de Ingenieros de Montes.
- Santamarta, J.C., Hernández, L., Rodríguez-Losada, J., 2010. Volcanic dikes engineering properties for storing and regulation of the underground water resources in volcanic islands. In: Olalla, C., Hernandez, L.E., Rodríguez-Losada, J.A., Peruchó, A., González-Gallego, J. (Eds.), *Rock Mechanics and Geo-Engineering in Volcanic Environments*. CRC Press, pp. 95–98. <https://doi.org/10.1201/B10549-14>.
- Schmork, S., Mercado, A., 1969. Upconing of fresh water—sea water interface below pumping wells, field study. *Water Resour. Res.* 5, 1290–1311. <https://doi.org/10.1029/WR005i006p01290>.
- Scholl, M.A., Ingebritsen, S.E., Janik, C.J., Kauahikaua, J.P., 1996. Use of precipitation and groundwater isotopes to interpret regional hydrology on a tropical Volcanic Island: Kilauea Volcano Area, Hawaii. *Water Resour. Res.* 32, 3525–3537. <https://doi.org/10.1029/95WR02837>.
- Sebben, M.L., Werner, A.D., Graf, T., 2015. Seawater intrusion in fractured coastal aquifers: a preliminary numerical investigation using a fractured Henry problem. *Adv. Water Resour.* 85, 93–108. <https://doi.org/10.1016/j.advwatres.2015.09.013>.
- Servando-Molowny, I., 1998. Estudio Hidrogeológico del Pozo de Los Padrones. Universidad de La Laguna.
- Simmons, C.T., Fenstemaker, T.R., Sharp, J.M., 2001. Variable-density groundwater flow and solute transport in heterogeneous porous media: approaches, resolutions and future challenges. *J. Contam. Hydrol.* 52, 245–275. [https://doi.org/10.1016/S0169-7722\(01\)00160-7](https://doi.org/10.1016/S0169-7722(01)00160-7).
- Stoeckl, L., Houben, G., 2012. Flow dynamics and age stratification of freshwater lenses: experiments and modeling. *J. Hydrol.* 458–459, 9–15. <https://doi.org/10.1016/j.jhydrol.2012.05.070>.
- Stoeckl, L., Houben, G.J., Dose, E.J., 2015. Experiments and modeling of flow processes in freshwater lenses in layered island aquifers: analysis of age stratification, travel times and interface propagation. *J. Hydrol.* 529, 159–168. <https://doi.org/10.1016/j.jhydrol.2015.07.019>.
- Strack, O.D.L., Stoeckl, L., Damm, K., Houben, G., Ausk, B.K., de Lange, W.J., 2016. Reduction of saltwater intrusion by modifying hydraulic conductivity. *Water Resour. Res.* 52, 6978–6988. <https://doi.org/10.1002/2016WR019037>.
- Takasaki, K.J., Mink, J.F., 1985. Evaluation of Major Dike-impounded Ground-water Reservoirs, Island of Oahu.
- Troll, V.R., Carracedo, J.C., 2016. In: Troll, V.R., Carracedo, J.C.B.T.-T.G. of the C.I. (Eds.), Chapter 2 - The Geology of El Hierro. Elsevier, pp. 43–99. <https://doi.org/10.1016/B978-0-12-809663-5.00002-5>.
- Vázquez-Suné, E., Marazuela, M.Á., Velasco, V., Diviu, M., Pérez-Estaún, A., Álvarez-Marrón, J., 2016. A geological model for the management of subsurface data in the urban environment of Barcelona and surrounding area. *Solid Earth* 7. <https://doi.org/10.5194/se-7-1317-2016>.
- Werner, A.D., Bakker, M., Post, V.E.A., Vandenbohede, A., Lu, C., Ataie-Ashtiani, B., Simmons, C.T., Barry, D.A., 2013. Seawater intrusion processes, investigation and management: recent advances and future challenges. *Adv. Water Resour.* 51, 3–26. <https://doi.org/10.1016/j.advwatres.2012.03.004>.
- Werner, A.D., Sharp, H.K., Galvis, S.C., Post, V.E.A., Sinclair, P., 2017. Hydrogeology and management of freshwater lenses on atoll islands: review of current knowledge and research needs. *J. Hydrol.* 551, 819–844. <https://doi.org/10.1016/j.jhydrol.2017.02.047>.
- Weymer, B.A., Everett, M.E., Haroon, A., Jegen-Kulcsar, M., Micallef, A., Berndt, C., Michael, H.A., Evans, R.L., Post, V., 2022. The coastal transition zone is an underexplored frontier in hydrology and geoscience. *Commun. Earth Environ.* 3, 1–8. <https://doi.org/10.1038/s43247-022-00655-8>.
- Younes, A., Fahs, M., 2015. Extension of the Henry semi-analytical solution for saltwater intrusion in stratified domains. *Comput. Geosci.* 19, 1207–1217. <https://doi.org/10.1007/s10596-015-9534-3>.
- Yu, X., Michael, H.A., 2019. Mechanisms, configuration typology, and vulnerability of pumping-induced seawater intrusion in heterogeneous aquifers. *Adv. Water Resour.* 128, 117–128. <https://doi.org/10.1016/j.advwatres.2019.04.013>.